SCIENCE CHINA
Chemistry

• ARTICLES •
• SPECIAL ISSUE • Chemical Methodology

January 2014 Vol.57 No.1: 141–146
doi: 10.1007/s11426-013-5008-4

Facile synthesis of size-tunable ZIF-8 nanocrystals using reverse micelles as nanoreactors

ZHAO XiaoJing[1], FANG XiaoLiang[2], WU BingHui[1], ZHENG LanSun[1] & ZHENG NanFeng[1*]

[1]*State Key Laboratory for Physical Chemistry of Solid Surfaces, Collaborative Innovation Center of Chemistry for Energy Materials; Department of Chemistry, College of Chemistry and Chemical Engineering, Xiamen University, Xiamen 361005, China*
[2]*Pen-Tung Sah Institute of Micro-Nano Science and Technology, Xiamen University, Xiamen 361005, China*

Received July 30, 2013; accepted August 27, 2013; published online October 31, 2013

This paper describes a robust method for the synthesis of high-quality ZIF-8 nanocrystals using reverse micelles as discrete nanoscale reactors. The precise size control of ZIF-8 nanocrystals is conveniently achieved by tuning the concentration of precursors, reaction temperatures, the amount of water, and the structure of surfactants. The as-synthesized ZIF-8 nanocrystals are of narrow distribution and tunable size. A size-dependent catalytic activity for Knoevenagel condensation reaction is further demonstrated by using ZIF-8 nanocrystals with different sizes as the catalysts. This facile method opens up a new opportunity in the synthesis of various ZIFs nanocrystals.

ZIF-8, nanocrystals, reverse micelles, catalysis

1 Introduction

Zeolitic imidazolate frameworks (ZIFs), a subclass of metal organic frameworks (MOFs), have been drawing increasing attention in the past decade [1]. ZIFs possess a zeolite topology, in which divalent metal cations are linked by imidazolate anions into tetrahedral frameworks. As one of the most studied prototypical ZIF compounds, ZIF-8 owns both large pores (11.6 Å) and small apertures (3.4 Å) [1, 2]. Together with its uniform porosity, the exceptional hydrothermal and chemical stabilities of ZIF-8 [3, 4] make it promising for many applications such as gas storage/separations [5–8], catalysis [9–15], supercapacitor [16–18], and chemical sensors [19–21]. As nanoscale MOFs exhibit unique physical and chemical properties distinctly from their corresponding bulk materials [22], the size- and morphology-controllable synthesis of ZIF-8 has opened new opportunities for its applications in catalysis [23], gas separation [5, 8] and the fabrication of hierarchically-structured materials [24]. Many methods have been developed for the synthesis of ZIF-8 microcrystals, such as electrospinning [25], ultrasound [26–28], self-template strategy [29, 30], and microwave [31]. To obtain ZIF-8 nanocrystals in organic [32–35] or aqueous solutions [36], the precursors (i.e. zinc nitrate hexahydrate and 2-methyl imidazole) are generally supplied in low concentrations. The size distributions of the obtained ZIF-8 nanocrystals were typically broad. The development of facile and effective strategies for preparing uniform ZIFs nanocrystals with controllable size is still challenging.

The surfactant-stabilized water-in-oil emulsions (i.e. reverse micelles) have been successfully used as spatially constrained nanoreactors for the controlled synthesis of various inorganic nanoparticles [37–40]. Since reverse micelles can provide homogeneous, isolated, and confined spaces for the crystal growth process, the nanoparticles synthesized by reverse micelles are uniform and highly dispersible. More importantly, the particle size can be further controlled by varying the structure of surfactants, the con-

*Corresponding author (email: nfzheng@xmu.edu.cn)

centration of precursors, the reaction temperatures, and the ratio of water/oil [40]. Lin *et al.* [41−43] have synthesized a series of MOF nanocrystals in a cetyltrimethylammonium bromide/isooctane/1-hexanol/water reverse microemulsion. To the best of our knowledge, ZIF-8 nanocrystals reported until now were mainly synthesized in the homogeneous solutions. Recently, we have developed a Brij C10/cyclohexane/water reverse micelle system to effectively coat noble metal nanoparticles with SiO_2 so that core-shell noble metal @SiO_2 nanoparticles can be yielded in high concentration [44, 45]. Such a facile and mild reverse micelle system provides a powerful platform for the controllable synthesis of nanomaterials [40].

Here, we report a facile, effective and scalable route to prepare high-quality ZIF-8 nanocrystals with uniform size and morphology. The rhombic dodecahedral ZIF-8 nanocrystals with narrow size distribution of 37 nm have been successfully synthesized by the Brij reverse micelle system. Simply by tuning the concentration of precursors, reaction temperatures, the amount of water, and the structure of surfactants, the size of as-synthesized ZIF-8 nanocrystals are controllable (30–160 nm). The size-dependent catalytic performance of ZIF-8 nanocrystals in the Knoevenagel reaction was demonstrated.

2 Experimental

2.1 Materials

$Zn(NO_3)_2·6H_2O$ (≥ 99.0%), cyclohexane, ethanol, methanol and tetrahydrofuran (THF) were purchased from Sinopharm Chemical Reagent Co., Ltd. 2-Methylimidazole (97%) was purchased from Alfa Aesar. Brij C10, Brij C20, and Brij 35 were purchased from Aldrich. Benzaldehyde, malononitrile, and *n*-dodecane were purchased from J&K Technology Co., Ltd. All chemicals were used as received without further purification. Deionized (DI) water was used in all experiments.

2.2 Synthesis

2.2.1 Synthesis of ZIF-8 nanocrystals in reverse micelles

In a typical procedure, Brij C10 (3.420 g), cyclohexane (15.0 mL) and an aqueous solution of $Zn(NO_3)_2·6H_2O$ (1.0 mL, 1.0 mol/L) were mixed under stirring at 37 °C to form a transparent reverse micelle solution A. Solution B was prepared under the same conditions except replacing Zn $(NO_3)_2·6H_2O$ with 2-methylimizadole (1.0 mL, 4.0 mol/L). Then solution B was rapidly added into solution A under stirring. The mixture turned turbid quickly. After stirring for 2 h, the product was separated with ethanol, centrifuged, and washed with ethanol for several times. A small part of the product was redispersed in ethanol to prepare samples for SEM and TEM measurements, and the other part of the product was dried in a vacuum drying oven at room-temperature overnight for other characterizations. The synthetic approach is highly reproducible and scalable.

2.2.2 Synthesis of ZIF-8 nanocrystals in water or CH_3OH

$Zn(NO_3)_2·6H_2O$ (1.0 mL, 1.0 mol/L) was added to 15.0 mL DI water. 2-Methylimidazole (1.0 mL, 4.0 mol/L) was added to another 15.0 mL DI water. The zinc nitrate solution was then mixed with the 2-methylimidazole solution under stirring. All the operations were performed at 50 °C. The mixture instantly turned milky after the two solutions mixed. After stirring for 2 h, the product was collected by centrifuging, and then washed with DI water for several times. The synthetic procedure in methanol was almost the same with the above conditions except replacing the water with methanol.

2.3 Catalysis studies

The Knoevenagel reaction between benzaldehyde and malononitrile using the ZIF-8 catalyst was carried out in a magnetically stirred round-bottom flask. A mixture of ZIF-8 (0.010 g), benzaldehyde (0.4 mL, 3.8 mmol), and *n*-dodecane (0.4 mL, 1.76 mmol) as an internal standard was placed into a 25 mL flask containing THF (8.0 mL). The reaction vessel was stirred for 5 min to disperse the ZIF-8 catalyst in the liquid phase. A solution of malononitrile (0.500 g, 7.6 mmol) in THF (2.0 mL) was then added, and the resulting mixture was stirred at room temperature. GC-MS was used to confirm the product identity. The reaction conversion was analyzed by gas chromatographic (GC).

2.4 Characterization

The phase of the products was characterized by X-ray powder diffraction (XRD, Panalytical X'pert PRO diffractometer with Cu-Kα radiation). Scanning electron microscopy (SEM) and transmission electron microscopy (TEM) images were taken on a Hitachi S-4800 microscope with a field-emission electron gun and a TECNAI F-30 high-resolution transmission electron microscope operating at 300 kV, respectively. The surface area of the as-synthesized ZIF-8 nanocrystals was measured by the Brunauer-Emmett-Teller (BET) method using nitrogen adsorption and desorption isotherms on a Micrometrics ASAP 2020 system. The pore size distribution plot was obtained by the Horvath-Kawazoe method. The dynamic light scattering (DLS) and zeta potential measurements were performed on Nano-ZS & MPT-2 (Malvern). Thermogravimetry analysis (TGA) was performed on a SDT-Q600 Thermoanalyzer. GC analyses were performed with a FuLi 9790II, equipped with a split/splitless injector, a capillary column (KB-5, 30 m × 0.32 mm × 0.33 μm) and a flame ionization detector.

3 Results and discussion

3.1 Synthesis of ZIF-8 nanocrystals in reverse micelles

The proposed procedure for the synthesis of ZIF-8 nanocrystals is shown in Scheme 1. Two separated reverse micelle solutions (A and B) were prepared using Brij C10, cyclohexane, and aqueous solution of the precursors. Reverse micelle solution A contained an aqueous solution of $Zn(NO_3)_2{\cdot}6H_2O$ while B contained an aqueous solution of 2-methylimidazole. After simply mixing reverse micelle A with B, uniform ZIF-8 nanocrystals were obtained.

Figure 1(a) shows the powder XRD pattern of the as-synthesized product. Compared with the simulated XRD pattern from the published ZIF-8 structure, the as-synthesized product can be indexed to pure-phase ZIF-8. All the diffraction peaks are obviously widened, suggesting the presence of small ZIF-8 nanocrystals in the product. The average size of the ZIF-8 nanocrystals deduced from Sherrer's formula for the strongest peak (110) is about 38 nm. The morphology of the as-synthesized ZIF-8 nanocrystals was further examined by TEM and SEM. As shown in Figure 1(b and c), the as-synthesized ZIF-8 nanocrystals are uniform rhombic dodecahedral particles with narrow size distribution. As measured from the SEM image, these particles have an average diameter of 37 nm, which agrees well with the result from the XRD pattern. The as-synthesized ZIF-8 nanocrystals can be dispersed in water to form stable suspensions. The photograph Figure 1(d) shows the typical Tyndall effect of the dispersed solution of as-synthesized ZIF-8 nanocrystals. The zeta potential value of the as-synthesized ZIF-8 is about +30 mV, indicating that the obtained nanocrystals can be stably dispersed in aqueous solution (Figure 1(e)). Indeed, the dispersed solution of the as-synthesized ZIF-8 nanocrystals was very stable. There was no sign of aggregated precipitation over 7 days (Figure 1(f)). To further demonstrate that the as-synthesized ZIF-8 nanocrystals are highly dispersible, the DLS technique is applied. As shown in Figure 1(g), the hydrodynamic diameters of the as-synthesized ZIF-8 nanocrystals possess a narrow size distribution with the peak value of 54 nm. These results have demonstrated that the proposed reverse micelle system is a facile and effective route to fabricate high-quality, uniform, and dispersible ZIF-8 nanocrystals.

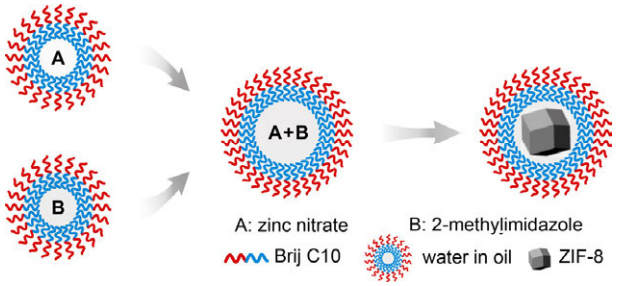

Scheme 1 Schematic illustration for the synthetic procedure of ZIF-8 nanocrystals in the reverse micelles.

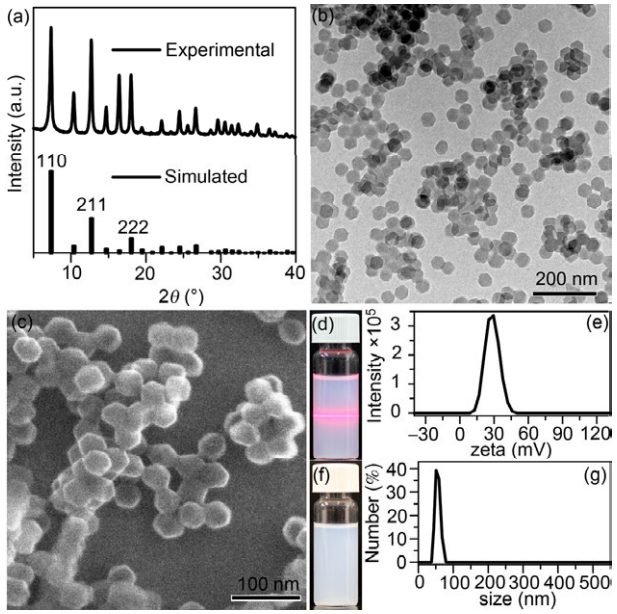

Figure 1 (a) XRD pattern, (b) TEM image, (c) SEM image, (d) photograph for the Tyndall effect; (e) zeta potential of the as-synthesized ZIF-8 nanocrystals; (f) photograph of the dispersed solution of the ZIF-8 nanocrystals aged for 7 days; (g) DLS curve of the as-synthesized ZIF-8 nanocrystals.

To further highlight the advantages of the confined space provided by proposed reverse micelle system, the syntheses of the ZIF-8 with the same concentration of precursors in water or methanol were carried out. As shown in Figure 2(a), the ZIF-8 particles obtained in aqueous system are mainly incomplete rhombic dodecahedra mixed with some irregular particles. These particles have a wide size distribution from several ten nanometers up to one micrometer. The poor morphology and broad size distribution can be attributed to the rapid reaction and growth process in aqueous system. In previous reports, due to its slow reaction and growth process, methanol was considered as a suitable solvent for the synthesis of well-shaped ZIF-8 nanocrystals in low concentration [33]. However, the rhombic dodecahedral ZIF-8 particles with an average diameter of 300 nm were obtained by using methanol as solvent (Figure 2(b)). Obviously, the intrinsic confined space of reverse micelle system provides a convenient route to synthesize nanoscale ZIF-8.

3.2 Size control of the ZIF-8 nanocrystals

Due to the inherent nature of reverse micelles, the as-

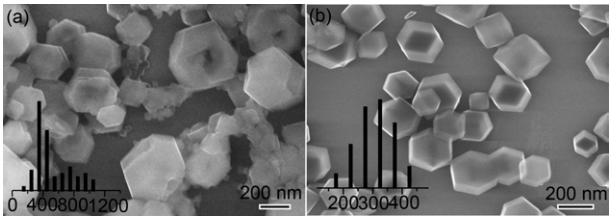

Figure 2 SEM images of ZIF-8 nanocrystals synthesized in (a) water and (b) methanol. Insets are the corresponding size distribution.

synthesized ZIF-8 nanocrystals are size-controllable. A series of experiments were carried out by varying each parameter of the reverse micelle system (i.e. reaction temperature, concentration of the precursors, and amount of water) while keeping all the other conditions the same. As shown in Figure 3 (a, b), the size of ZIF-8 nanocrystals decreased from 37 nm to 32 nm when the reaction temperature was changed from 50 °C to 37 °C. Decreasing the amount of the precursors led to the formation of smaller ZIF-8 nanocrystals. When the concentration of the precursors was decreased from 1.0 mol/L to 0.5 mol/L, the diameter of the nanocrystals was reduced to 28 nm (Figure 3(c)). As shown in Figure 3(d), when the volume of the aqueous solution of the precursors was reduced to 0.5 mL, the ZIF-8 nanocrystals with an average diameter of 130 nm were obtained.

The size of the ZIF-8 nanocrystals can also be tuned by changing the structure of surfactants. When nanocrystal growth is confined in isolated reverse micelles, the size of the micelle affects the dimension of final product. Therefore, a small reverse micelle size usually favors the formation of nanocrystals with a small size [40]. Compared with Brij C10, Brij C20 and Brij 35 have longer PEG portion and thus can form larger reverse micelles. As shown in Figure 4, when only replacing Brij C10 with Brij C20 or Brij®35 under the same reaction conditions, the average sizes of as-synthesized ZIF-8 were 51 nm and 164 nm, respectively. Based on these results, we believe that the choice of surfactants with different lengths of hydrophilic PEG segment is an effective route to control the synthesis of the ZIF-8 nanocrystals.

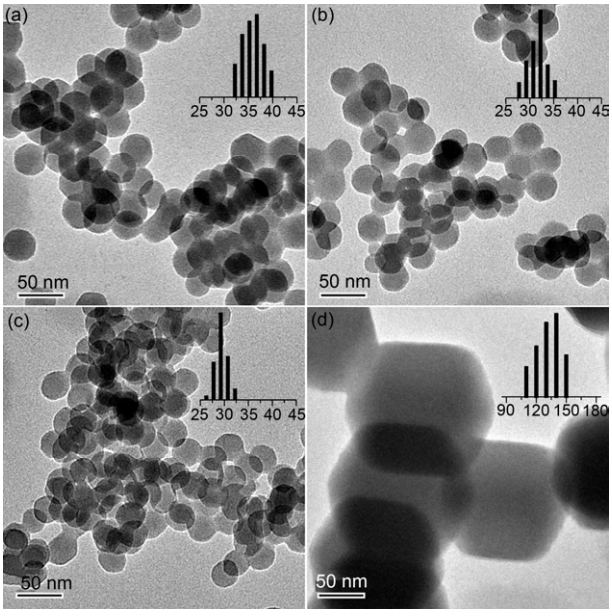

Figure 3 Synthesis of the ZIF-8 nanocrystals under different reaction conditions. (a) 50 °C, $Zn(NO_3)_2{\cdot}6H_2O$ (1.0 mL, 1.0 mol/L), 2-methylimizadole (1.0 mL, 4.0 mol/L); (b) 37 °C, $Zn(NO_3)_2{\cdot}6H_2O$ (1.0 mL, 1.0 mol/L), 2-methylimizadole (1.0 mL, 4.0 mol/L); (c) 37 °C, $Zn(NO_3)_2{\cdot}6H_2O$ (1.0 mL, 0.5 mol/L), 2-methylimizadole (1 mL, 2 mol/L); (d) 37 °C, Zn $(NO_3)_2{\cdot}6H_2O$ (0.5 mL, 1.0 mol/L), 2-methylimizadole (0.5 mL, 4.0 mol/L).

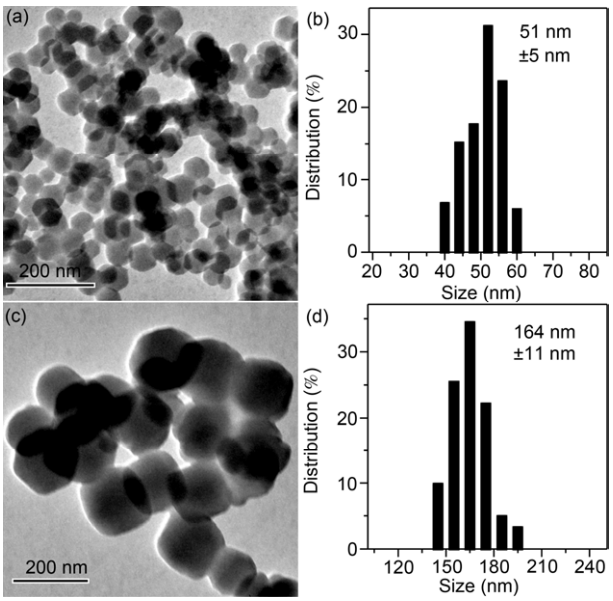

Figure 4 Synthesis of the ZIF-8 nanocrystals using different surfactants. (a) Brij C20 ($C_{16}H_{33}EO_{20}$); (c) Brij 35 ($C_{12}H_{25}EO_{23}$); (b, d) are the corresponding size distributions of ZIF-8 nanocrystals shown in (a, c).

3.3 Surface area and TGA analysis of ZIF-8 nanocrystals

The porosity of the as-synthesized ZIF-8 nanocrystals (37 nm) was investigated by N_2 adsorption–desorption measurements. As shown in Figure 5(a), the as-synthesized ZIF-8 nanocrystals exhibit a type I isotherm. While the significant increase in the adsorbed volume at very low relative pressures is due to the presence of micropores, the second uptake at high relative pressure indicates the presence of textural meso/macroporosity formed by packing of nanoparticles. The microporous volume is about 0.58 cm^3/g and the BET area is 1478.5 cm^2/g. This BET area is larger than the ZIF-8 nanocrystals reported by Lai *et al.* (1079 cm^2/g) [36] and Michael Wiebcke *et al.* (962 cm^2/g) [33]. The pore distribution of the as-synthesized ZIF-8 nanocrystals (37 nm) was obtained from the analysis of the adsorption branch of the isotherm by the Horvath-Kawazoe calculations. As shown in Figure 5(b, c), ZIF-8 nanocrystals have a narrow pore-size distribution at approximately 1.1 nm, which agrees very well with the micropore size of the ZIF-8 bulk materials.

Figure 5(c) shows the TGA curve of the ZIF-8 nanocrystals (37 nm) performed under nitrogen flow. The TGA curve exhibit a gradual weight loss step of 10.8% up to 250 °C, corresponding to the removal of guest molecules (e.g. H_2O) from the cavities or residual species (e.g. 2-methylimidazole) from the surface of the nanocrystals [36]. A long plateau was observed in the temperature range of 250–550 °C, indicating high thermal stability of the sample. To further confirm thermal stability, the ZIF-8 nanocrystals were treated at 500 °C under N_2 atmosphere for 2 hours. As shown in Figure 5(d), the thermally treated ZIF-

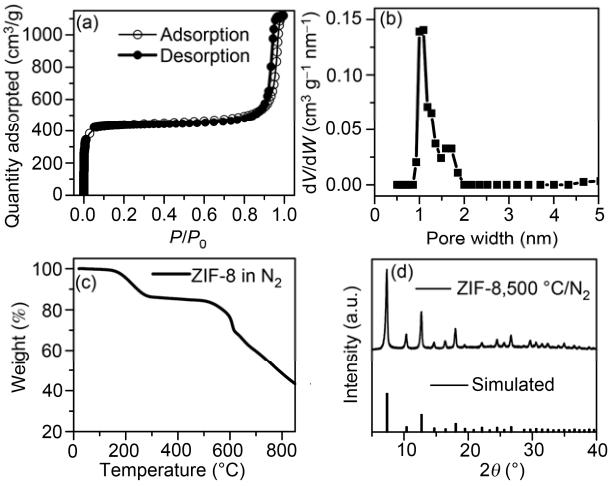

Figure 5 N_2 absorption isotherms (a), pore-size distribution (b), and TGA curve (c) of the as-synthesized ZIF-8 nanocrystals; (d) XRD pattern of ZIF-8 nanocrystals calcined in N_2 at 500 °C for 2 hours.

8 nanocrystals showed no change in the XRD pattern. The crystallite size of the thermally treated ZIF-8 nanocrystals calculated from the corresponding XRD pattern is about 40 nm, demonstrating that the ZIF-8 nanocrystals synthesized in this work have good thermal stability.

3.4 Catalytic activity of different sizes ZIF-8 nanocrystals for Knoevenagel reaction

The Knoevenagel condensation of aldehydes with compounds containing activated methylene groups is one of the most useful and widely employed methods for carbon-carbon bond formation with numerous applications in the synthesis of fine chemicals [46] as well as heterocyclic compounds of biological significance [47]. Recently, Chizallet *et al*. [48] have described that ZIF-8 has significant activity for the trans-esterification of vegetable oil due to the acid sites of Zn^{2+} and the basic sites of N^- moieties and OH groups. Based on the available basic sites, ZIF-8 exhibits efficient activity for the Knoevenagel reaction at low temperature. As the six-membered ring pore windows of the ZIF-8 are as narrow as 3.4 Å, larger molecules can not enter the pore cavities. It is thus reasonable to propose that the Knoevenagel condensation reaction of benzaldehyde with malononitrile mainly occurs on the external surface of ZIF-8 [49]. We thus explored their catalytic performance in the Knoevenagel reaction using ZIF-8 nanocrystals with different sizes as the catalysts (Scheme 2). Before use, the catalysts were pretreated at 400 °C for two hours to remove surfactants on the surface. As shown in Table 1, it was found that increasing the particle size of the ZIF-8 nanocrystals resulted in a significant drop in reaction rate. Conversions of 91.9%, 80.1%, and 68.3% were obtained after 0.5 h reaction using 1.25 mol% ZIF-8 with particle sizes of 37, 135, and 300 nm, respectively. The results indicate that smaller ZIF-8 nanocrystals exhibit higher catalytic activity due to the increased external surface of the smaller crystals.

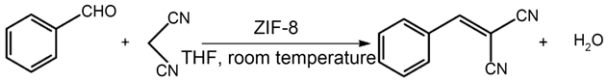

Scheme 2 Knoevenagel condensation reaction of benzaldehyde with malononitrile using the ZIF-8 catalyst.

Table 1 Size-dependent catalytic activity of ZIF-8 for Knoevenagel reaction

Entry	Size of ZIF-8 (nm)	*t* (h)	Conversion (%)
1	37	0.5	91.9
2	135	0.5	80.1
3	300	0.5	68.3

4 Conclusions

In summary, we have reported a robust method to synthesize size-controllable ZIF-8 nanocrystals using reverse micelles as nanoreactors. ZIF-8 nanocrystals with uniform morphology and size were successfully obtained by the Brij/cyclohexane/water reverse micelle system. The size of the as-synthesized ZIF-8 nanocrystals can be tuned by controlling the reaction temperature, the concentration of the precursors, the amount of water, and the structure of surfactants. Moreover, we have demonstrated that ZIF-8 nanocrystals with the smaller size exhibit higher activity for Knoevenagel reaction. The facile, large-scale production of ZIF-8 nanocrystals with high uniformity and size tunability makes them promising candidates for further designing noble metal/ZIF-8 hybrid nanomaterials for sensing and catalytic application.

We thank the financial support from the Ministry of Science and Technology of China (2011CB932403), and the National Natural Science Foundation of China (21131005, 21333008, 20925103, 21021061).

1 Park KS, Ni Z, Cote AP, Choi JY, Huang R, Uribe-Romo FJ, Chae HK, O'Keeffe M, Yaghi OM. Exceptional chemical and thermal stability of zeolitic imidazolate frameworks. *Proc Natl Acad Sci*, 2006, 103: 10186–10191
2 Huang XC, Lin YY, Zhang JP, Chen XM. Ligand-directed strategy for zeolite-type metal-organic frameworks: Zinc(II) imidazolates with unusual zeolitic topologies. *Angew Chem Int Ed*, 2006, 45: 1557–1559
3 Banerjee R, Phan A, Wang B, Knobler C, Furukawa H, O'Keeffe M, Yaghi OM. High-throughput synthesis of zeolitic imidazolate frameworks and application to CO_2 capture. *Science*, 2008, 319: 939–943
4 Phan A, Doonan CJ, Uribe-Romo FJ, Knobler CB, O'Keeffe M, Yaghi OM. Synthesis, structure, and carbon dioxide capture properties of zeolitic imidazolate frameworks. *Acc Chem Res*, 2010, 43: 58–67
5 Demessence A, Boissiere C, Grosso D, Horcajada P, Serre C, Ferey G, Soler-Illia GJAA, Sanchez C. Adsorption properties in high optical quality nanoZIF-8 thin films with tunable thickness. *J Mater Chem*, 2010, 20: 7676–7681
6 Wang B, Cote AP, Furukawa H, O'Keeffe M, Yaghi OM. Colossal cages in zeolitic imidazolate frameworks as selective carbon dioxide reservoirs. *Nature*, 2008, 453: 207–211
7 Li LM, Wang HF, Yan XP. Metal-organic framework ZIF-8

nanocrystals as pseudostationary phase for capillary electrokinetic chromatography. *Electrophoresis*, 2012, 33: 2896–2902
8 Chang N, Gu ZY, Yan XP. Zeolitic imidazolate framework-8 nanocrystal coated capillary for molecular sieving of branched alkanes from linear alkanes along with high-resolution chromatographic separation of linear alkanes. *J Am Chem Soc*, 2010, 132: 13645–13647
9 Jiang HL, Liu B, Akita T, Haruta M, Sakurai H, Xu Q. Au@ZIF-8: CO oxidation over gold nanoparticles deposited to metal-organic framework. *J Am Chem Soc*, 2009, 131: 11302–11303
10 Zhu MQ, Srinivas D, Bhogeswararao S, Ratnasamy P, Carreon MA. Catalytic activity of ZIF-8 in the synthesis of styrene carbonate from CO_2 and styrene oxide. *Catal Commun*, 2013, 32: 36–40
11 Lu G, Li S, Guo Z, Farha OK, Hauser BG, Qi X, Wang Y, Wang X, Han S, Liu X, DuChene JS, Zhang H, Zhang Q, Chen X, Ma J, Loo SC, Wei WD, Yang Y, Hupp JT, Huo FW. Imparting functionality to a metal-organic framework material by controlled nanoparticle encapsulation. *Nat Chem*, 2012, 4: 310–316
12 Karagiaridi O, Lalonde MB, Bury W, Sarjeant AA, Farha OK, Hupp JT. Opening ZIF-8: A catalytically active zeolitic imidazolate framework of sodalite topology with unsubstituted linkers. *J Am Chem Soc*, 2012, 134: 18790–18796
13 Dang TT, Zhu Y, Ngiam JSY, Ghosh SC, Chen A, Seayad AM. Palladium nanoparticles supported on ZIF-8 as an efficient heterogeneous catalyst for aminocarbonylation. *ACS Catal*, 2013, 3: 1406–1410
14 Kuo CH, Tang Y, Chou LY, Sneed BT, Brodsky CN, Zhao Z, Tsung CK. Yolk-shell nanocrystal@ZIF-8 nanostructures for gas-phase heterogeneous catalysis with selectivity control. *J Am Chem Soc*, 2012, 134: 14345–14348
15 Li Z, Zeng HC. Surface and bulk integrations of single-layered Au or Ag nanoparticles onto designated crystal planes {110} or {100} of ZIF-8. *Chem Mater*, 2013, 25: 1761–1768
16 Torad NL, Hu M, Kamachi Y, Takai K, Imura M, Naito M, Yamauchi Y. Facile synthesis of nanoporous carbons with controlled particle sizes by direct carbonization of monodispersed ZIF-8 crystals. *Chem Commun*, 2013, 49: 2521–2523
17 Chaikittisilp W, Hu M, Wang H, Huang HS, Fujita T, Wu KC, Chen LC, Yamauchi Y, Ariga K. Nanoporous carbons through direct carbonization of a zeolitic imidazolate framework for supercapacitor electrodes. *Chem Commun*, 2012, 48: 7259–7261
18 Wang Q, Xia W, Guo W, An L, Xia D, Zou R. Functional zeolitic-imidazolate-framework-templated porous carbon materials for CO capture and enhanced capacitors. *Chem Asian J*, 2013, 8(8): 1879–1885
19 Lu G, Hupp JT. Metal-organic frameworks as sensors: A ZIF-8 based Fabry-Perot device as a selective sensor for chemical vapors and gases. *J Am Chem Soc*, 2010, 132: 7832–7833
20 Kreno LE, Leong K, Farha OK, Allendorf M, Van Duyne RP, Hupp JT. Metal-organic framework materials as chemical sensors. *Chem Rev*, 2012, 112: 1105–1125
21 Liu S, Xiang ZH, Hu Z, Zheng XP, Cao DP. Zeolitic imidazolate framework-8 as a luminescent material for the sensing of metal ions and small molecules. *J Mater Chem*, 2011, 21: 6649–6653
22 Lin W, Rieter WJ, Taylor KM. Modular synthesis of functional nanoscale coordination polymers. *Angew Chem Int Ed*, 2009, 48: 650–658
23 Miralda CM, Macias EE, Zhu M, Ratnasamy P, Carreon MA. Zeolitic imidazole framework-8 catalysts in the conversion of CO_2 to chloropropene carbonate. *ACS Catal*, 2012, 2: 180–183
24 Cao AM, Hu JS, Wan LJ. Morphology control and shape evolution in 3D hierarchical superstructures. *Sci China Chem*, 2012, 55: 2249–2256
25 Fan LL, Xue M, Kang ZX, Li H, Qiu SL. Electrospinning technology applied in zeolitic imidazolate framework membrane synthesis. *J Mater Chem*, 2012, 22: 25272–25276
26 Cho HY, Kim J, Kim SN, Ahn WS. High yield 1-L scale synthesis of ZIF-8 via a sonochemical route. *Micropor Mesopor Mat*, 2013, 169: 180–184
27 Ge D, Lee HK. Sonication-assisted emulsification microextraction combined with vortex-assisted porous membrane-protected micro-solid-phase extraction using mixed zeolitic imidazolate frameworks 8 as sorbent. *J Chromatogr A*, 2012, 1263: 1–6
28 Seoane B, Zamaro JM, Tellez C, Coronas J. Sonocrystallization of zeolitic imidazolate frameworks (ZIF-7, ZIF-8, ZIF-11 and ZIF-20). *Crystengcomm*, 2012, 14: 3103–3107
29 Zhu MQ, Venna SR, Jasinski JB, Carreon MA. Room-temperature synthesis of ZIF-8: The coexistence of ZnO nanoneedles. *Chem Mater*, 2011, 23: 3590–3592
30 Zhan WW, Kuang Q, Zhou JZ, Kong XJ, Xie ZX, Zheng LS. Semiconductor@metal-organic framework core-shell heterostructures: A case of ZnO@ZIF-8 nanorods with selective photoelectrochemical response. *J Am Chem Soc*, 2013, 135: 1926–1933
31 Kwon HT, Jeong HK. Highly propylene-selective supported zeolite-imidazolate framework (ZIF-8) membranes synthesized by rapid microwave-assisted seeding and secondary growth. *Chem Commun*, 2013, 49: 3854–3856
32 Cravillon J, Nayuk R, Springer S, Feldhoff A, Huber K, Wiebcke M. Controlling zeolitic imidazolate framework nano- and microcrystal formation: Insight into crystal growth by time-resolved in situ static light scattering. *Chem Mater*, 2011, 23: 2130–2141
33 Cravillon J, Munzer S, Lohmeier SJ, Feldhoff A, Huber K, Wiebcke M. Rapid room-temperature synthesis and characterization of nanocrystals of a prototypical zeolitic imidazolate framework. *Chem Mater*, 2009, 21: 1410–1412
34 Cravillon J, Schroder CA, Nayuk R, Gummel J, Huber K, Wiebcke M. Fast nucleation and growth of ZIF-8 nanocrystals monitored by time-resolved *in situ* small-angle and wide-angle X-ray scattering. *Angew Chem Int Ed*, 2011, 50: 8067–8071
35 Nune SK, Thallapally PK, Dohnalkova A, Wang C, Liu J, Exarhos GJ. Synthesis and properties of nano zeolitic imidazolate frameworks. *Chem Commun*, 2010, 46: 4878–4880
36 Pan YC, Liu YY, Zeng GF, Zhao L, Lai ZP. Rapid synthesis of zeolitic imidazolate framework-8 (ZIF-8) nanocrystals in an aqueous system. *Chem Commun*, 2011, 47: 2071–2073
37 Pileni MP. Reverse micelles as microreactors. *J Phys Chem*, 1993, 97: 6961–6973
38 Riter RE, Willard DM, Levinger NE. Water immobilization at surfactant interfaces in reverse micelles. *J Phys Chem B*, 1998, 102: 2705–2714
39 Woo K, Lee HJ, Ahn JP, Park YS. Sol-gel mediated synthesis of Fe_2O_3 nanorods. *Adv Mater*, 2003, 15: 1761–1764
40 Gao CB, Lu ZD, Yin YD. Gram-scale synthesis of silica nanotubes with controlled aspect ratios by templating of nickel-hydrazine complex nanorods. *Langmuir*, 2011, 27: 12201–12208
41 Rieter WJ, Taylor KM, An H, Lin WB. Nanoscale metal-organic frameworks as potential multimodal contrast enhancing agents. *J Am Chem Soc*, 2006, 128: 9024–9025
42 Taylor KM, Jin A, Lin WB. Surfactant-assisted synthesis of nanoscale gadolinium metal-organic frameworks for potential multimodal imaging. *Angew Chem Int Ed*, 2008, 47: 7722–7725
43 Taylor KM, Rieter WJ, Lin WB. Manganese-based nanoscale metal-organic frameworks for magnetic resonance imaging. *J Am Chem Soc*, 2008, 130: 14358–14359
44 Chen C, Fang XL, Wu BH, Huang LJ, Zheng NF. A multi-yolk-shell structured nanocatalyst containing sub-10 nm Pd nanoparticles in porous CeO_2. *ChemCatChem*, 2012, 4: 1578–1586
45 Liu ZH, Fang XL, Chen C, Zheng NF. Pd nanoparticles encapsulated in hollow mesoporous aluminosilica nanospheres as an efficient catalyst for multistep reactions and size-selective hydrogenation. *Acta Chim Sinica*, 2013, 71: 334–338
46 Freeman F. Properties and reactions of ylidenemalononitriles. *Chem Rev*, 1980, 80: 329–350
47 Tietze LF. Domino reactions in organic synthesis. *Chem Rev*, 1996, 96: 115–136
48 Chizallet C, Lazare S, Bazer-Bachi D, Bonnier F, Lecocq V, Soyer E, Quoineaud AA, Bats N. Catalysis of transesterification by a nonfunctionalized metal-organic framework: Acido-basicity at the external surface of ZIF-8 probed by FTIR and ab initio calculations. *J Am Chem Soc*, 2010, 132: 12365–12377
49 Tran UPN, Le KKA, Phan NTS. Expanding applications of metal-organic frameworks: Zeolite imidazolate framework ZIF-8 as an efficient heterogeneous catalyst for the Knoevenagel reaction. *ACS Catal*, 2011, 1: 120–127